Digest Journal of Nanomaterials and Biostructures Vol. 6, No 3, July - September 2011, p. 1273-1279

FROM NANOSCALE ENGINEERING TO BIOMEDICAL APPLICATION - CHARACTERIZATION OF PULSE ELECTRODEPOSITED BIOMIMETIC ANTIBACTERIAL COATING ON Ti_6Al_4Zr

C. UNGUREANU, D. IONITA, N.BADEA, I. DEMETRESCU*
"Politehnica" University of Bucharest, Bucharest, Romania

The paper aim is to prepare using fast pulse electrodeposition a new type of biomimetic coating with hydroxiapatite (HA) and silver nanoparticles (nAg) on Ti6Al4Zr alloy.The hydroxiapatite acts as an agent of osseointegration and silver nanoparticles have an antibacterial effect. Silver nanoparticles were characterized using dynamic light scattering instrument to determine the size distribution. The electrodeposition takes place at 40°C and the electrolyte was an aqueous solution of $Ca(NO_3)_2$ and $NH_4H_2PO_4$. HA/Ag nanocomposite coatings were prepared by adding $AgNO_3$ and cysteine in electrolyte. The morphological and elemental analysis of the new coating on the Ti6Al4Zr surface were performed with scanning electron microscopy (SEM), transmission electro microscopy (TEM) and energy disperse spectroscopy (EDS). Antibacterial activity was evaluated from the inhibition of *Escherichia coli* bacteria.

(Received June 17, 2011; accepted August 30, 2011)

Keywords: electrodeposition, biomimetic coating, antibacterial effect, Ti_6Al_4Zr

1. Introduction

The old concept that implant materials should present a "biotolerant" surface in order to minimize immune and fibrotic responses, is changed. In the approach that implanted substrates should not only provide structural support for damaged tissues, but also integrate with these tissues, biomimetic coatings which may promote regeneration are more and more interesting for tissue engineering [1, 2]. However, despite the problems of Hydroxyapatite (HA) weak adherence to the metallic substrate [3, 4], the system HA and titanium (or titanium alloys) are now more than ever used as coatings for joint replacement implants and dental implants due to various surface treatments before or after its deposition which may assure mechanical properties [5, 6].

Such systems promote better bone ingrowth. between the joint implant and the patient's bone itself, HA being a component of bone with very high biocompatibility. The procedures of enhancing bioperformace of biomimetic coatings were intensively proposed and investigated in the last decade [7-9]. One strategy was related to functionalization of HA coatings [7] in order to stimulate cell adhesion and help oseointegation and HA modified with various peptides [8, 9] was subject of many papers and debats [9]. This evolution in thinking has prompted a burgeoning effort to engineer substrates in order to assure performance for short, medium and long term.

A key starting point for designing the implant succes is related to to reduce the incidence of implant-associated infections, taking into account that bacteria growth are more and more agressive. In this spirit, introducing composites coatings and nanoparticles with antibacterial effect [10-13], is a significant and topical field of research, as well as fabrication and characterization of nanoparticles with bactericidal potential [14, 15]. We report in the present paper elaboration and characterization of a new type of biomimetic coating with hydroxiapatite (HA) and silver nanoparticles on Ti6Al4Zr bioalloy using fast pulse electrodeposition. Having both biomimetic

*Corresponding author: i_demetrescu@chim.upb.ro

and antibacterial components this coating simultaneously provides excellent antibacterial activity and osteointegration.

2. Experimental

2.1. Surface samples preparation

Prior to electrodeposition, the Ti_6Al_4Zr surfaces were mechanically ground to 1000-grit SiC paper. Then passivation was performed by immersing in 40% nitric acid for 30 min. They were used as the substrates for the thin (TiO_2/TiAlZr). These specimens were washed in distilled water by ultrasonic cleaning for 15 min.

Then they went through alkali treatments to increase hydrophilicity, which was performed by immersing specimens in 100 mL of 5.0 mol l^{-1} NaOH aqueous solution at 60 ^oC for 24 h. Finally, the specimens were washed with distilled water and dried in air.

2.2.Preparation of HA/Ag composite coatings

Pure HA coating on Ti_6Al_4Zr and doped HA coating with silver ions, were prepared by pulsed electrochemical deposition method. Electrodeposition was carried out in a standard three-electrode cell in which a Pt foil was used as auxiliary (counter) electrode and a saturated calomel electrode (SCE) as reference electrode. The electrolyte was prepared by dissolving of 5 mmol L^{-1} $Ca(NO_3)_2$ and 3 mmol L^{-1} $NH_4H_2PO_4$.at 40^oC in Millipore water. This solution was sonicated in an ultrasonic bath (35 kHz, 100 W) at 40^oC. Pulse electrodeposition was conducted with a pulse width of 100 s at − 1.5 V, for 2h. HA/Ag composite coatings were prepared by adding 1mM $AgNO_3$ and cysteine into the electrolyte witch acted as the coordination agent to stabilize Ag ions. Under continuous stirring, the pH was adjusted to 9 by adding drop wise a 1M NaOH aqueous solution to precipitate Ag^+ cations as Ag_2O, according to the potential-pH diagram in aqueous solution for silver [16]. After deposition, the Ti plates with coatings were rinsed with deionized water and dried in air at 60 °C for 2h. Finally, the specimens went through heat treatments at 800 ^oC for 1h. There are two types of coverage obtained: HA with out Ag (HA/TiAlZr) and HA/Ag composite coating (Ag-HA/TiAlZr).

2.3 Characterization of nanoparticle dispersed in electrolyte.

Dynamic light scattering (Zetasizer Nano ZS, Malvern Instruments Ltd., U.K.), was used to determine the size distribution of particles by measuring dynamic fluctuations of light scattering intensity caused by the Brownian motion of the particles. The measurement gives as a result the average hydrodynamic diameter of the particles, the peak values in the hydrodynamic diameter distribution and the polydispersity index (PdI) that describes the width of particle size distribution. The PdI scale ranges from 0 to 1 (with 0 being monodisperse and 1 being polydisperse). All measurements were carried out in triplicate with a temperature equilibration time of 1 minute at 25 ^oC. The data processing mode was set to high multi-modal resolution.

2.4.Characterization of coating

SEM analysis

The aspect and structure of the coatings formed on the metallic surfaces were studied by scanning electron microscopy (SEM) with Environmental Scanning Electron Microscope FEI/Phillips XL 30 (ESEM) at a pressure of 0.7 torrs working way GSE (water vapours). EDX analyses were performed to identify the elemental composition at specific locations on the surface.

TEM analysis

Nanosized particles are investigated using TEM analysis (transmission electron microscopy) with an EM-410 Philips, 60 kV microscope.

2.5.Electrochemical test

Dynamic potential polarization curves were acquired from the TiO_2/TiAlZr, HA/TiAlZr and Ag-HA/TiAlZr samples in Hank solution using Volta lab 21 equipment. The measurement was conducted using a conventional three-electrode electrochemical cell with a saturated calomel electrode (SCE) as the reference electrode, a Pt as the counter electrode, and the sample with a

$1cm^2$ exposed area as the working electrode. Prior to the polarization test, the samples were stabilized in the solution for 15 min and the tests were conducted at room temperature at a scanning rate 2 mV/sec. The testing solution was Hank bioliquid with the following composition: 9 g/L NaCl, 0.24 g/L $CaCl_2$, 0.43 g/L KCl and 0.2 g/L $NaHCO_3$.

2.6. Evaluation of antibacterial activity

For antibacterial activity evaluation three sterile samples were used as following:

Escherichia coli (K 12-MG1655) was aerobically cultured in a tube containing Luria Bertani (LB) medium at 37 ^oC. The initial concentration of bacteria was adjusted to 10^{-9} colony forming units (CFU)/mL by dilution with sterile water.

A quantitative analysis using 10^{-9} CFU of a gram negative bacterium which were cultured on LB agar plates containing: TiO_2/TiAlZr, HA/TiAlZr; Ag-HA/TiAlZr

LB agar plates with *E. coli* cultured under the same conditions were used as a control.

Four microliters of bacterial solution was pipetted onto each specimen. A sterile glass was placed over the specimen and the bacterial solution. After 3h, the specimen and sterile glass were transferred to a 10 mL of sterile water, and then fully vibrated (Disruptor Genie vortex) in order to harvest the cells. 1 mL of each rinse was placed onto Bacto-Agar plates.

The plates were incubated for 24 hours at 37 ^oC, and the numbers of colonies were counted.

The antibacterial effect in each group was represented by the bactericidal ratio, which was calculated as follows:

$$\text{Bactericidal ratio}(\%) = \frac{CFU_{\text{control group}} - CFU_{\text{experimental group}}}{CFU_{\text{control group}}} \cdot 100 \quad (1)$$

The counts on the three plates corresponding to each sample were averaged.

3.Results and discussion

3.1. Characterization of nanoparticles obtained in electrolyte

The granulometric analysis of electrolyte after sonication (without silver, Figure 1a) revealed a stretch size distribution of HA particles with an average size of 137 nm with good polydispersity (Pdi= 0.217±0.015).

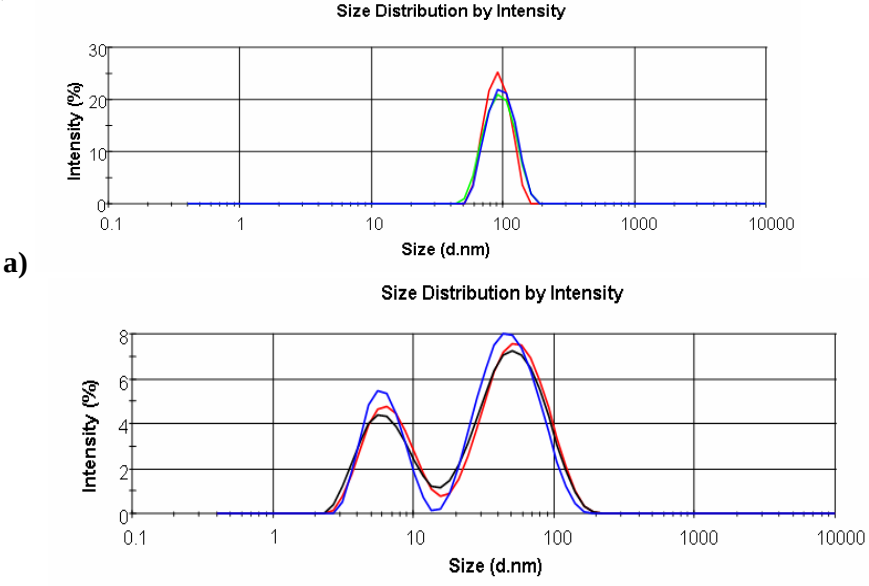

Fig 1. Size distribution of nanopaticle in electrolyte. a) after sonication b) after ading $AgNO_3$

$AgNO_3$ addition changes the DLS spectrum. Particles distribution for the electrolyte in which has been added $AgNO_3$ and cysteine shows two peaks: one of them corresponding to Ag nanoparticles and the other to hydroxyapatita nanoparticles that were aggregated Ag nanoparticles.

According to DLS analysis, the size of Ag nanoparticles is between 5 and 30 nm which is consistent with TEM analysis.

As can be seen in Figure 1a, Ag nanoparticles sizes have much smaller diameters comparing to HA.

3.2. SEM analysis

TiAlZr coated with HA

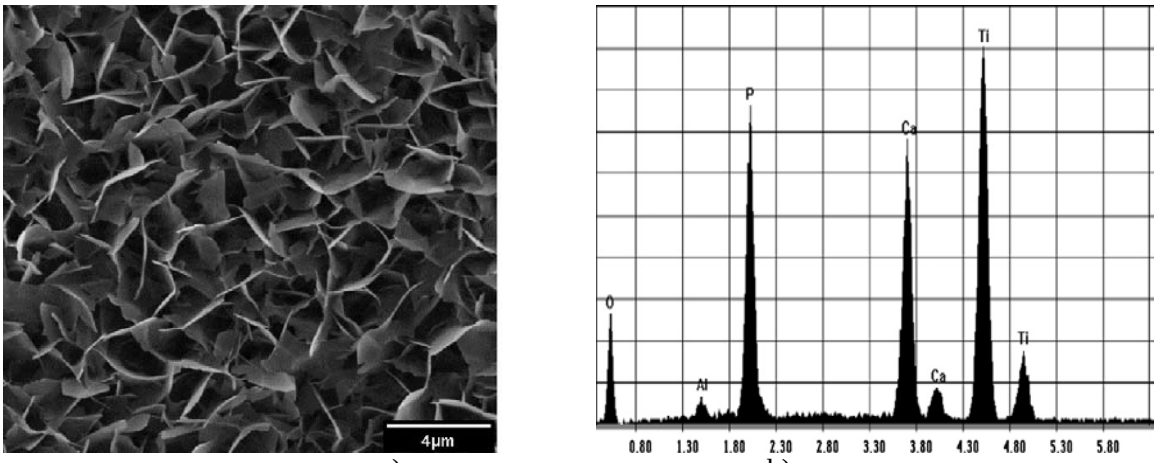

a) b)

Fig 2. SEM image (a) and EDS spectrum (b) of HA/TiAlZr

After puls electrodeposition without $AgNO_3$ the TiAlZr surface area was completely covered by a thick Ca–P layer exhibiting the tell tale rose-like morphology observed as shown in Fig. 2a.

The EDS spectrum for TiAlVZr alloy after electrodeposition of HA is presented in Figure 3b. Chemical elemental analysis of the HA coating detected oxygen, aluminum, phosphor, calcium, and titanium as the main constituent elements, indicating that the coating is complex deposit on the alloy surface. The Ca/P ratio obtained on the surface was 1.64, almost the same value as the one of the hydroxyapatite (1.67), confirming the formation of the hydroxyapatite.

TiAlVZr coated with Ag-HA.

The morphology of the HA/Ag coatings was revealed by SEM micrographs (Figure 3a). EDS line prdile analysis was conducted in order to investigate Ag distribution in the film. The results proved that Ag was uniformly distributed in the film. The chemical elements of the Ag–HA film deposited on titanium were Ca, P, Ti, O and Ag. The Ca/P ratio obtained on the surface was 1.62.

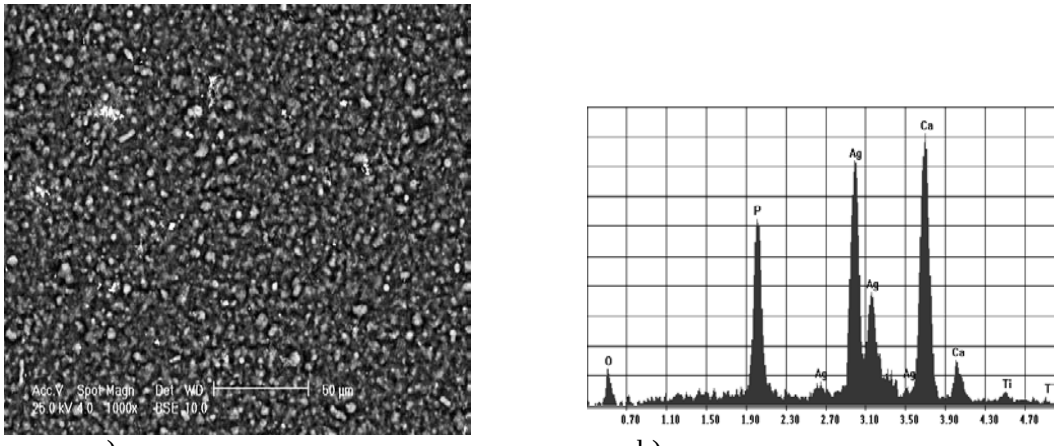

a) b)

Fig. 3. SEM image (a) and EDS spectrum (b) of Ag- HA/TiAlZr

3.3. TEM analysis

SEM data are in concordance with TEM image which confirms the attachment of silver nanoparticles on HA. Figure 4 shows the TEM image of the HA modified with silver particles.

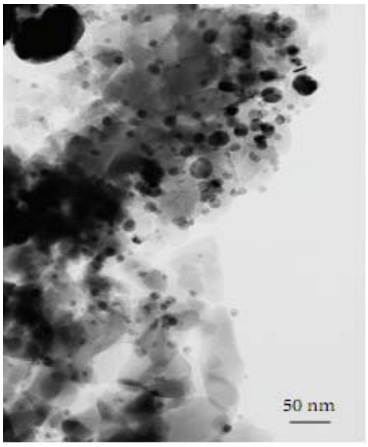

Fig. 4. TEM micrograph of silver nanoparticles loaded on hydroxyapatite.

TEM images show a size distribution of globular-shape silver particles that range between less than 10 nm and 60 nm. It can be seen that the silver particles preferentially adhere to the surfaces of HA. Dark little spots corresponds to Ag nanoparticles and larger spots corresponds to HA. The density of attached nanocrystals is high. Observed silver particles appear to have a narrow size distribution, and no free particles are observed in the background of the TEM images, which confirms all formed Ag nanoparticles are durably attached to the HA.

3.4.Electrochemical behavior

The alloy covered with Ag-HA/TiAlZr exhibited lower corrosion rates than the alloy covered with HA, denoting the better efficiency of the Ag-HA coating in Hank solution. According to table 1 with electrochemical parameters (where E_{cor} is corrosion potential, I_{cor}, is corrosion current density and R_p polarization resistance) this behavior is sustained firstly by E_{cor} which is shifted to more electropositive values in this case. The corrosion rate for Ag-HA/TiAlZr coated specimen is 28.9 times lower then TiO_2/TiAlZr and such values support the better anticorrosive properties of coating.

Table 1.Electrochemical parameters for TiO_2/TiAlZr, HA/TiAlZr, Ag-HA/TiAlZr

Samples	E_{cor} (mV)	I_{cor} ($\mu A/cm^2$)	R_p($K\Omega cm^2$)	V_{cor} ($\mu m/y$)
TiO_2/TiAlZr	-307	25.75	127.08	497.53
HA/TiAlZr	-246	15.68	76.56	308.02
Ag-HA/TiAlZr	-67	0.88	26.44	17.17

3.5.Antimicrobial activity

In Fig. 5 are presented the plates incubated for 24 h at 37 ^oC to determine the number of viable *E. coli* in terms of CFU.

TiO_2/TiAlZr

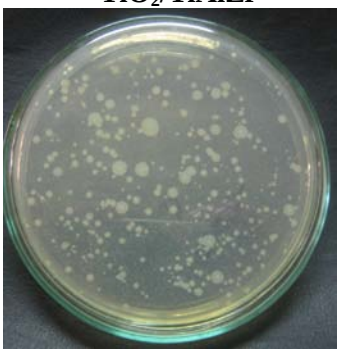

- no dilution

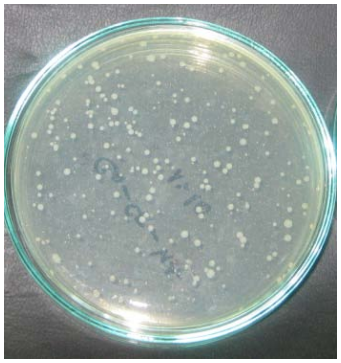

- 1:10 dilution

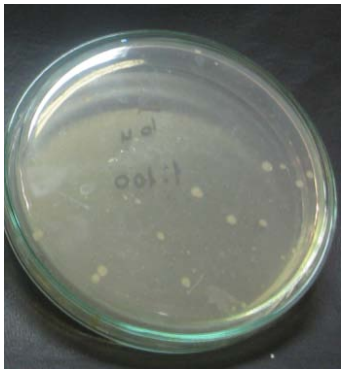

- 1:100 dilution

HA/TiAlZr

- no dilution

- 1:10 dilution

- 1:100 dilution

Ag-HA/TiAlZr

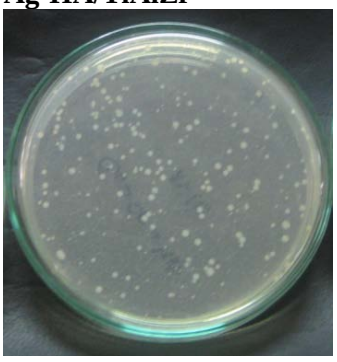

- no dilution

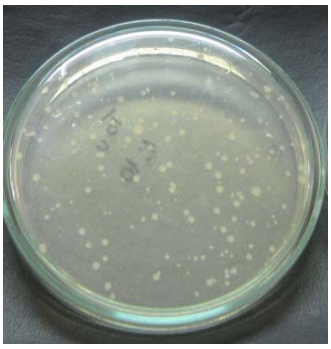

- 1:10 dilution

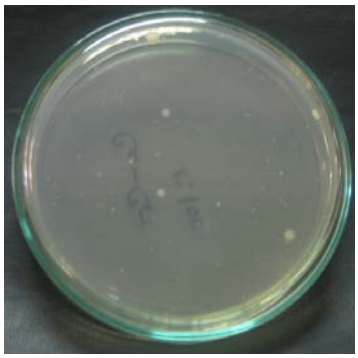

- 1:100 dilution

Fig. 5. Bacto-Agar plates with CFU of E. coli to determine the antibacterial effects

After 24 hours, the presence of $TiAlZr/TiO_2$ inhibited the bacterial growth by 22% ($560 \cdot 10^3$ CFU/mL). In the presence of TiAlZr/HA was counted $250 \cdot 10^3$ CFU/mL with a inhibition a bacterial growth by 65%, while presence of Ag-Ha/TiAlZr caused 92% inhibition of bacterial growth ($56 \cdot 10^3$ CFU/mL). For Control plate was counted $720 \cdot 10^3$ CFU/mL. According to above data bacterial ratio is increasing as following TiO_2/TiAlZr, HA /TiAlZr Ag-HA/TiAlZr.

The bactericidal activity results show that this nanocomposite is strongly active against the gram negative bacteria strain, so it can be considered as an antimicrobial biomaterial.

Regarding the Ag antibacterial activity mechanism against *Escherichia coli* bacteria [17, 18], in the literature the effect of Ag^+ ions was distinguished from that of nanosilver particles. The

antibacterial activity of nanosilver was predominated by Ag^+ ions when Ag nanoparticles with aproximately 10 nm diameter were employed. The interfacial interactions of bacteria on metal nanoparticles involve Ag^+ ions action according to a type Troyan horse mechanism [19]. In contrast, when relatively larger Ag nanoparticles were used, the concentration of the released Ag^+ ions was lower sustaining size dependent bactericidal activity [20]. Smaller nanoparticles as reported in this paper, have larger surface area and have greater antibacterial effect [21].

4. Conclusions

The data suggest that the new type of biomimetic coating with hydroxiapatite (HA) and silver nanoparticle nAg on TiAlZr bioalloy can be elaborated via a fast pulse electrodeposition method.

Electrochemical parameters from dynamic polarization tests performed in Hank solution indicate better anticorrosive properties for the TiAlZr alloy after the pulse electrodeposition of biomimetic coating nAg-HA.

The bacteriological experiments performed in vitro demonstrated efficacy of new biomimetic coating nAg-HA. on TiAlZr implants against growth of *Escherichia coli* bacteria.

Acknowledgements

This work was supported by CNCSIS –UEFISCSU, project number PNII – IDEI PCCE 248/2010.

References

[1] Y. Liu, G. Wu, K. de Groot, J. R. Soc. Interface doi 10.1098/rsif.2010.0115 (2010).
[2] C. Berbecaru, H.V. Alexandru, A. Ianculescu, A. Popescu, G. Socol, F. Sima, I. Mihailescu, Appl. Surf. Sci. **255**, 5476, (2009).
[3] H. Wie, H. Herø, T. Solheim, E. Kleven, A.M. Rørvik, H.R. Haanaes, J. Biomed. Mater. Res. **29**(11), 1443, (1995).
[4] S.-H. Lee, H.-W. Kim, E.-J. Lee, L.-H.Li, H.-E. Kim, J. Biomater. Appl. **20** (3), 195 (2006).
[5] G.P. Dinda, J. Sshin, J. Mazumder, Acta Biomater. **5** (5),1821 (2009).
[6] H.-W. Kim, Y.-H. Koh, L.-H. Li, S. Lee and H.-E. Kim, Biomaterials **25** (13), 2533 (2004).
[7] S. Piskounova, J. Forsgren, U. Brohede, H. Engqvist, M. Strømme, Journal of Biomedical Materials Research, Part B: Applied Biomaterials **91** (2), 780 (2009).
[8] S. Roessler, R. Born, D. Scharnweber, H. Worch, A. Sewing, M. Dard, J. Mater. Sci. Mater. Med. **12** (10-12), 871 (2001).
[9] S. L .Bellis, Biomaterials **32** (18), 4205 (2011).
[10] W. Chen, Y. Liu, H. S. Courtney, M. Bettenga, C. M. Agrawal, J. D. Bumgardner and J. L. Ong, Biomaterials. **27** (32), 5512 (2006).
[11] Z. L Shi, P. H., Chua, K. G. Neoh, E. T Kang, W.Wang, Int. J. Artif. Organs **31**,777 (2008).
[12] A. Panácek, L. Kvítek, R. Prucek, R. Kolár, M. Vecerová, N. Pizúrová, Silver J PhysChemB **10**, 16248 (2006).
[13] J. Luo, W.-B. Chan, L. Wang and C.-J. Zhong, Int. J. Antimicrob. Agents. **36** (6), 549 (2010).
[14] M. Popescu, A. Velea, A. Lorinczi, Digest J. Nanomat. Biostruct. **5**, 1035 (2010).
[15] P. Prema, R. Raju, Biotechnology and Bioproces Engineering **14** (6), 842 (2009).
[16] M. Pourbaix, Atlas of Electrochemical Equilibria in Aqueous Solutions, National Association of Corrosion Engineers, Houston, Tex, (1974)
[17] A. G. Sotiriou, E. Sotiris Pratsinis, Sci. Technol. **44** (14), 5649 (2010).
[18] J. Luo, W.-B. Chan, L. Wang and C.-J. Zhong, Int. J. Antimicrob. Agents **36** (6), 549 (2010).
[19] E.-J. Park, J. Yi, Y. Kim, K. Choi, K. Park, Toxicology in Vitro **24,** 872 (2010).
[20] A. Panacek, L. Kvitek, R. Prucek, M. Kolar, R. Vecerova, N. Pizurova, V.K. Sharma, T. Nevecna, R. Zboril, J Phys Chem B. **110** (33), 16248 (2006).
[21] N. Lkhgvajav, I. Yasa, E. Celik, M. Koizhaganova, O. Sari, Digest J. Nanomat. Biostruct. **6** (1), 149 (2011).